PeerJ Preprints NOT PEER-REVIEWED

TITLE: Zika virus impairs growth in human neurospheres and brain organoids

SUMMARY: We provide evidence that Zika virus infects human iPS-derived neural stem cells, causing cell death and reduced growth in neurospheres and cerebral organoids.

AUTHORS: Patricia P. Garcez [2,1,@], Erick Correia Loiola[1*], Rodrigo Madeiro da Costa[1*], Luiza M. Higa[3*], Pablo Trindade [1*], Rodrigo Delvecchio[3], Juliana Minardi Nascimento[1,4], Rodrigo Brindeiro[3], Amilcar Tanuri[3], Stevens K. Rehen[1, 2, @]

AFFILIATIONS:

[1] D'Or Institute for Research and Education (IDOR), Rio de Janeiro, Brazil

[2] Institute of Biomedical Sciences, Federal University of Rio de Janeiro, Rio de Janeiro, Brazil

[3] Institute of Biology, Federal University of Rio de Janeiro, Rio de Janeiro, Brazil

[4] Institute of Biology, State University of Campinas (UNICAMP), Campinas, Brazil.

[*]Authors contributed equally to this work.

[@]Corresponding authors: S.K.R. (srehen@lance-ufrj.org) and/or P.P.G. (ppgarcez@gmail.com)

PeerJ Preprints | https://doi.org/10.7287/peerj.preprints.1817v3 | CC-BY 4.0 Open Access | rec: 13 Mar 2016, publ: 13 Mar 2016

PeerJ Preprints NOT PEER-REVIEWED

ABSTRACT

Since the emergence of Zika virus (ZIKV), reports of microcephaly have increased dramatically in Brazil; however, causality between the widespread epidemic and malformations in fetal brains has not been confirmed. Here, we examine the effects of ZIKV infection in human neural stem cells growing as neurospheres and cerebral organoids. Using immunocytochemistry and electron microscopy, we show that ZIKV targets human brain cells, reducing their viability and growth as neurospheres and cerebral organoids. These results suggest that ZIKV abrogates neurogenesis during human brain development.

MAIN TEXT:

Primary microcephaly is a severe malformation characterized by the reduction of brain size during embryonic development. Patients display a heterogeneous range of brain impairments, compromising motor, visual, hearing and cognitive functions (*1*).

Microcephaly is associated with decreased neuronal production as a consequence of proliferative defects and death of cortical progenitor cells (*2*). During pregnancy, the primary etiology of microcephaly varies from genetic mutations to external insults. The so-called TORCHS factors (Toxoplasmosis, Rubella, Cytomegalovirus, Herpes virus, Syphilis) are the main congenital infections that compromise brain development *in utero* (*3*).

The dramatic increase in the rate of microcephaly in Brazil has been associated with the recent outbreak of Zika virus (ZIKV) (*4*), a flavivirus that is transmitted by mosquitoes

PeerJ Preprints | https://doi.org/10.7287/peerj.preprints.1817v3 | CC-BY 4.0 Open Access | rec: 13 Mar 2016, publ: 13 Mar 2016

(*5*), and sexually (*6-8*). So far, ZIKV has been described in the placenta and amniotic fluid of microcephalic fetuses (9-12), and in the blood of microcephalic newborns (10,13). ZIKV had also been detected within the brain of a microcephalic fetus (12,13), however, there is no direct evidence that ZIKV causes brain malformations.

Here we used human induced pluripotent stem (iPS) cells cultured as neural stem cells (NSC), neurospheres and brain organoids to explore the consequences of ZIKV infection to neurogenesis.

Human iPS-derived NSCs were infected with ZIKV (MOI 0.25 to 0.025). After 24 hours, ZIKV was detected in NSCs (**Figure 1A-D**), when viral envelope protein was present between 3.0% (MOI 0.025) and 8.4% (MOI 0.25) of the cell population exposed to ZIKV (**Figure 1E**). The virus RNA was also detected in these NSC cultures with qRT-PCR (**Figure 1F**), suggesting these cells supports productive infection.

In order to investigate the effects of ZIKV during neural differentiation, mock- and ZIKV-infected NSCs were cultured as neurospheres. After 3 days *in vitro*, mock NSCs generated round neurospheres. However, ZIKV-infected NSCs generated neurospheres with morphological abnormalities and cell detachment (**Figure 2B**). After 6 days *in vitro* (DIV), hundreds of neurospheres have grown under mock conditions (**Figure 2C and 2E**). Strikingly, in ZIKV-infected NSCs (MOI 0.25 to 0.025) only a few neurospheres survived (**Figure 2D and 2E**).

Mock neurospheres present the expected ultrastructural morphology of nucleus and mitochondria (**Figure 3A**). ZIKV-infected neurospheres revealed the presence of viral particles (**Figure 3C-F,** arrows), similarly to the observed in murine glial and neuronal

PeerJ Preprints | https://doi.org/10.7287/peerj.preprints.1817v3 | CC-BY 4.0 Open Access | rec: 13 Mar 2016, publ: 13 Mar 2016

cells (*14*). ZIKV was bound to the membranes as well as in mitochondria and vesicles of cells within infected neurospheres (**Figure 3B-F**). Apoptotic nuclei, a hallmark of cell death, were observed in all ZIKV-infected neurospheres analyzed (**Figure 3B**). Of note, ZIKV-infected cells in neurospheres presented smooth membrane structures (SMS) (**Figure 3B and 3F**), similar to previously described in other cell types infected with the dengue virus (*15*). These results suggest that ZIKV induces cell death in human neural stem cells, which impairs the formation of neurospheres.

To further investigate the impact of ZIKV infection during neurogenesis, human iPS-derived cerebral organoids (16) were infected with ZIKV, and followed by 11 days *in vitro* (**Figure 4**). The growth rate of 12 individual organoids (6 per condition) was measured during this period (**Figure 4A-D**). As a result of ZIKV infection, the average growth area of ZIKV-infected organoids was reduced by 40% when compared to brain organoids under mock conditions (0.624 mm^2 ± 0.064 ZIKV-infected organoids versus 1.051 mm^2 ± 0.1084 mock-infected organoids normalized, **Figure 4E**).

Altogether, our results demonstrate that ZIKV induces cell death in human iPS-derived neural stem cells, disrupts the formation of neurospheres and reduces the growth of brain organoids (**Figure 5**).

Cell death impairing brain enlargement, incidence of calcifications and microcephaly is well described in congenital infections with TORCHS (17-19). Our results, together with the recent reports showing brain calcifications in microcephalic fetuses and newborns infected with ZIKV (9,13) reinforce the growing body of evidence connecting congenital ZIKV outbreak to the increased number of reports about brain malformations in Brazil.

PeerJ Preprints | https://doi.org/10.7287/peerj.preprints.1817v3 | CC-BY 4.0 Open Access | rec: 13 Mar 2016, publ: 13 Mar 2016

METHODS:

All protocols and procedures were approved by the institutional research ethics committee of Hospital Copa D'Or (CEPCOPADOR) under # 727.269.

Human iPS cells

Human induced pluripotent stem cells (20) were cultured either on Essential 8 medium (Thermo Fisher Scientific, USA) containing DMEM/F12 and supplement, or mTeSR1 (Stemcell Technologies, USA) on Matrigel (BD Biosciences, USA) coated surface. The colonies were manually passaged every 5-7 days until they reached 70-80% confluence and maintained at 37°C in humidified air with 5% CO_2.

Neural stem cells

Human iPS cells were split and 24h hours later medium was switched to PSC neural Induction Medium (Thermo Fisher Scientific, USA), containing Neurobasal medium and PSC supplement, according to manufacturer's protocol (21). Medium was changed every other day until day 7, when initial neural stem cells (NSC) are split and expanded on neural induction medium (Advanced DMEM/F12 and Neurobasal medium (1:1) with neural induction supplement; Thermo Fisher Scientific, USA).

Formation of neurospheres

PeerJ Preprints | https://doi.org/10.7287/peerj.preprints.1817v3 | CC-BY 4.0 Open Access | rec: 13 Mar 2016, publ: 13 Mar 2016

Neural stem cells (NSC) were cultured until 80% confluence and split with Accutase (Merck-Millipore, Germany). NSCs were resuspended in neural differentiation medium with half DMEM/F12 and half Neurobasal medium supplemented with 1X N2 and 1X B27 supplements. The suspended NSC cells were grown under rotation at 90 rpm, and medium was replaced every 4 days. Pictures were acquired using with EVOS Cell Imaging System (Thermo Fisher Scientific, USA).

Formation of cerebral organoids

The differentiation into cerebral organoids was based in a previously described protocol (16). Briefly, human iPS cells were dissociated and inoculated into a spinner flask containing a final volume of 50 mL of mTeSR1 supplemented with 10 µM Y-27632 (Rho-associated protein kinases inhibitor, iRock) (Merck-Millipore, Germany) under rotation at 40 rpm. After 24h, the medium was changed to Dulbecco's modified eagle medium (DMEM)/F12, supplemented with 20% KnockOut™ Serum Replacement (KOSR), 2 mM Glutamax, 1% MEM non-essential amino acids (MEM-NEAA), 55 µM 2-Mercaptoethanol and 100 U/mL Penicillin-Streptomycin (Thermo Fisher Scientific, USA). By day 6, embryoid bodies were fed with neural induction media (DMEM/F12, 1x N2 supplement, 2 mM Glutamax, 1% MEM-NEAA and 1 µg/mL heparin (Sigma, USA) for 5 days. On day 11, cellular aggregates were embedded in Matrigel for 1h at 37°C and 5% CO_2. Then, medium was changed to 1:1 DMEM/F12: Neurobasal, 0.5x N2, 1x B27 minus vitamin A, 2 mM Glutamax, 0.5% MEM-NEAA, 0.2 µM 2-Mercaptoethanol and

PeerJ Preprints | https://doi.org/10.7287/peerj.preprints.1817v3 | CC-BY 4.0 Open Access | rec: 13 Mar 2016, publ: 13 Mar 2016

2.5 µg/mL insulin. After 4 days, cell aggregates were grown in neuronal differentiation media, composed as aforementioned except by replacing with B27 containing vitamin A (Thermo Fisher Scientific, USA). The medium was changed every week. Organoids were grown until 35 days under these conditions. Organoids were infected with ZIKV. Pictures were acquired using with EVOS Cell Imaging System (Thermo Fisher Scientific, USA). Areas of individual organoids were measured with ImageJ.

Infection of cells with ZIKV

ZIKV strain MR766 (a kind gift of Dr. Davis F. Ferreira, Federal University of Rio de Janeiro, Brazil) was propagated in Vero cells. Briefly, cells were either mock or ZIKV-infected. At 48 hours post infection (hpi), cytopathic effect was observed and conditioned media from mock and ZIKV-infected cells were harvested, centrifuged at 300 x g and stored at -80^{o}C. ZIKV genome was sequenced and strain identity was confirmed (accession number NC_012532). ZIKV titers were determined by plaque assay performed in Vero cells 5 x 10^7 PFU/ml and diluted 1:100, 1:1000 and 1:10,000 (MOI ranging from 0.0025 to 0.25) to infect NSC and neurospheres or 1:100 and 1:10,000 in organoids experiments. Cells were incubated with virus or mock for 2 hours, when medium containing virus particles was replaced with fresh medium. NSCs were analyzed 24 hours post-infection. Neurospheres were formed after the infection of NSC, and then grown until the 6th day. Organoids were infected with ZIKV (3 x 10^2 to 3 x 10^4 PFU) or mock on day 35 *in vitro*, and further incubated for 11 days until analysis.

PeerJ Preprints | https://doi.org/10.7287/peerj.preprints.1817v3 | CC-BY 4.0 Open Access | rec: 13 Mar 2016, publ: 13 Mar 2016

PeerJ Preprints NOT PEER-REVIEWED

RNA extraction and RT-PCR

RNA from mock and ZIKV-infected NSCs supernatants were extracted using QIAamp Viral RNA Mini Kit according to manufacturer's instructions. Reverse transcription-polymerase chain reaction (RT-PCR) was performed as a rapid molecular tool to detect viral infection in acute-phase samples using ZIKV primers 1086, 1162 and probe 1107 FAM described elsewhere using TaqMan® One-Step RT-PCR Master Mix Reagents Kit (22).

Electron microscopy

ZIKV-infected neurospheres were immersed in formalin for biosafety reasons. Then, neurospheres were immersed in fixative solution containing 2.5% glutaraldehyde (v/v), 0.1 M Na-cacodylate buffer (pH 7.2). All samples were post fixed in 1% OsO_4 in cacodylate buffer plus 5 mM calcium chloride and 0.8% potassium ferricyanide, dehydrated in acetone and embedded in EPON. Ultrathin sections (70 nm) were collected on 300 mesh copper grids, stained with uranyl acetate and lead citrate and observed at 80 Kv with a Zeiss 900 transmission electron microscope.

Immunostaining

NSCs were seeded in 3.5 x 10^4 cells/cm^2 cell density on 96-multiwell Cell-Carrier plates (PerkinElmer, USA) covered with 10 µg/mL poly-L-ornithine (Sigma-Aldrich, USA) overnight and 2.5 µg/mL laminin for 3 hours. After 24 hours, cells were fixed with 4%

PeerJ Preprints | https://doi.org/10.7287/peerj.preprints.1817v3 | CC-BY 4.0 Open Access | rec: 13 Mar 2016, publ: 13 Mar 2016

paraformaldehyde (Sigma-Aldrich, USA) in phosphate-buffered saline for 15 min, permeabilized with 0.3% Triton X-100 (Sigma-Aldrich, USA), treated with 50 mM ammonium chloride, followed by blocking with 3% bovine serum albumin (Sigma-Aldrich, USA) and overnight incubation with rabbit anti-human-Sox2 (1:100; Merck-Millipore, Germany) and mouse anti-flavivirus group antigen antibody (clone 4G2, 1:100) (23). Subsequently, samples were incubated with the following secondary antibodies: goat anti-rabbit AlexaFluor 488 IgG (1:400; Thermo Fischer Scientific, USA) and goat anti-mouse Alexa Fluor 594 IgG (1:400; Thermo Fischer Scientific, USA). Nuclei were stained with 0.5 µg/mL 4′-6-diamino-2-phenylindole (DAPI) for 5 min. Images were acquired on Operetta high-content imaging system with a 20x objective, high numerical apertures (NA) (PerkinElmer, USA). Total number of cells was calculated by nuclei stained with DAPI. Analysis of data was performed using the image analysis software Harmony 5.1 (PerkinElmer, USA). Seven different fields from duplicate wells per experimental condition were used for quantification. Representative images were acquired on a confocal microscope (TCS SP8, Leica, Germany).

Statistical analysis

Data are expressed as mean ± SEM. Statistical analyses were performed using unpaired two-tailed Student's t-test with Prism software, version 6. *$p < 0.05$, **$p < 0.01$, ***$p<0.001$.

REFERENCES:

PeerJ Preprints | https://doi.org/10.7287/peerj.preprints.1817v3 | CC-BY 4.0 Open Access | rec: 13 Mar 2016, publ: 13 Mar 2016

PeerJ Preprints NOT PEER-REVIEWED

1. Gilmore EC, Walsh CA. Genetic causes of microcephaly and lessons for neuronal development. Wiley Interdisciplinary Reviews: …. 2013.

2. Woods CG, Bond J, Enard W. Autosomal Recessive Primary Microcephaly (MCPH): A Review of Clinical, Molecular, and Evolutionary Findings. The American Journal of Human Genetics. Elsevier; 2005 May 1;76(5):717–28.

3. Neu N, Duchon J, Zachariah P. TORCH Infections. Clinics in Perinatology. 2015 Mar;42(1):77–103.

4. Campos GS, Bandeira AC, Sardi SI. Zika virus outbreak, Bahia, Brazil. Emerging Infect Dis. 2015.

5. Hayes EB. Zika Virus Outside Africa. Emerging Infect Dis. 2009 Sep;15(9):1347–50.

6. Dick GWA. Zika virus. II. Pathogenicity and physical properties. Trans R Soc Trop Med Hyg. 1952 Sep;46(5):521–34.

7. Musso D, Roche C, Robin E, Nhan T, Teissier A, Cao-Lormeau V-M. Potential sexual transmission of Zika virus. Emerging Infect Dis. 2015 Feb;21(2):359–61.

8. Foy BD, Kobylinski KC, Chilson Foy JL, Blitvich BJ, Travassos da Rosa A, Haddow AD, et al. Probable non-vector-borne transmission of Zika virus, Colorado, USA. Emerging Infect Dis. 2011 May;17(5):880–2.

PeerJ Preprints | https://doi.org/10.7287/peerj.preprints.1817v3 | CC-BY 4.0 Open Access | rec: 13 Mar 2016, publ: 13 Mar 2016

9. Sarno M, Sacramento GA, Khouri R, do Rosario MS, Costa F, Archanjo G, et al. Zika Virus Infection and Stillbirths: A Case of Hydrops Fetalis, Hydranencephaly and Fetal Demise. PLOS Negleted Tropical Diseases. 2016 Feb 25;1–5.

10. Calvet G, Aguiar RS, Melo ASO, Sampaio SA, de Filippis I, Fabri A, et al. Articles Detection and sequencing of Zika virus from amniotic fluidof fetuses with microcephaly in Brazil: a case study. The Lancet Infectious Diseases [Internet]. Elsevier Ltd; 2016 Feb 16;:1–8. Available from: http://www.sciencedirect.com/science/article/pii/S1473309916000955

11. Oliveira Melo AS, Malinger G, Ximenes R, Szejnfeld PO, Alves Sampaio S, Bispo de Filippis AM. Zika virus intrauterine infection causes fetal brain abnormality and microcephaly: tip of the iceberg? Ultrasound Obstet Gynecol. 2016 Jan 5;47(1):6–7.

12. Martines RB, Bhatnagar J, Keating MK, Silva-Flannery L, Muehlenbachs A, Gary J, et al. Notes from the Field: Evidence of Zika Virus Infection in Brain and Placental Tissues from Two Congenitally Infected Newborns and Two Fetal Losses — Brazil, 2015. MMWR Morb Mortal Wkly Rep. 2016 Feb 19;65(06):159–60.

13. Mlakar J, Korva M, Tul N, Popović M, Poljšak-Prijatelj M, Mraz J, et al. Zika Virus Associated with Microcephaly. N Engl J Med. 2016 Feb 10;:160210140106006.

PeerJ Preprints | https://doi.org/10.7287/peerj.preprints.1817v3 | CC-BY 4.0 Open Access | rec: 13 Mar 2016, publ: 13 Mar 2016

14. Bell TM, Field EJ, Narang HK. Zika virus infection of the central nervous system of mice. Archiv für die gesamte Virusforschung. 1971.

15. Grief C, Galler R, Côrtes LMC, Barth OM. Intracellular localisation of dengue-2 RNA in mosquito cell culture using electron microscopic in situ hybridisation. Arch Virol. Springer-Verlag; 1997 Mar 7;142(12):2347–57.

16. Lancaster MA, Renner M, Martin C-A, Wenzel D, Bicknell LS, Hurles ME, et al. Cerebral organoids model human brain development and microcephaly. Nature. 2013 Sep 19;501(7467):373–9.

17. Neu N, Duchon J, Zachariah P. TORCH infections. Clinics in Perinatology. 2015.

18. Naing ZW, Scott GM, Shand A, Hamilton ST, van Zuylen WJ, Basha J, et al. Congenital cytomegalovirus infection in pregnancy: a review of prevalence, clinical features, diagnosis and prevention. Aust N Z J Obstet Gynaecol. 2016 Feb;56(1):9–18.

19. Vasconcelos-Santos DV, Machado Azevedo DO, Campos WR, Oréfice F, Queiroz-Andrade GM, Carellos ÉVM, et al. Congenital Toxoplasmosis in Southeastern Brazil: Results of Early Ophthalmologic Examination of a Large Cohort of Neonates. Ophthalmology. 2009 Nov;116(11):2199–2205.e1.

20. Paulsen BDS, Cardoso SC, Stelling MP, Cadilhe DV, Rehen SK. Valproate reverts zinc and potassium imbalance in schizophrenia-derived reprogrammed cells. Schizophr Res. 2014 Apr;154(1-3):30–5.

PeerJ Preprints | https://doi.org/10.7287/peerj.preprints.1817v3 | CC-BY 4.0 Open Access | rec: 13 Mar 2016, publ: 13 Mar 2016

21. Yan Y, Shin S, Jha BS, Liu Q, Sheng J, Li F, et al. Efficient and rapid derivation of primitive neural stem cells and generation of brain subtype neurons from human pluripotent stem cells. Stem Cells Transl Med. 2013 Oct 25;2(11):862–70.

22. Lanciotti RS, Kosoy OL, Laven JJ, Velez JO, Lambert AJ, Johnson AJ, et al. Genetic and Serologic Properties of Zika Virus Associated with an Epidemic, Yap State, Micronesia, 2007. Emerging Infect Dis. 2008 Aug;14(8):1232–9.

23. Henchal EA, Gentry MK, McCown JM, Brandt WE. Dengue virus-specific and flavivirus group determinants identified with monoclonal antibodies by indirect immunofluorescence. Am J Trop Med Hyg. 1982 Jul 31.

ACKNOWLEDGEMENTS: The authors thank the lab-crew members Marcelo Costa, Ismael Gomes, Gabriela Vitória and Matías Alloati for providing technical support, cultures of human iPS cells and brain organoids. Authors also thank Fabricio Pamplona, Mind the Graph and CENABIO.

Funding: Funds (not specifically for Zika virus studies) were provided by the Brazilian Development Bank (BNDES); Funding Authority for Studies and Projects (FINEP); and fellowships from the National Council of Scientific and Technological Development (CNPq); Foundation for Research Support in the State of Rio de Janeiro (FAPERJ); São Paulo Research Foundation (FAPESP); Coordenação de Aperfeiçoamento de Pessoal de Nível Superior (CAPES).

PeerJ Preprints | https://doi.org/10.7287/peerj.preprints.1817v3 | CC-BY 4.0 Open Access | rec: 13 Mar 2016, publ: 13 Mar 2016

Competing interests: The authors declare no competing financial interests.

PeerJ Preprints | https://doi.org/10.7287/peerj.preprints.1817v3 | CC-BY 4.0 Open Access | rec: 13 Mar 2016, publ: 13 Mar 2016

FIGURE LEGENDS:

Fig. 1. ZIKV infects human neural stem cells

Confocal microscopy images of iPS-derived NSCs double stained for (**A**) ZIKV in the cytoplasm, and (**B**) Sox2 in nuclei, one day after virus infection. (**C**) DAPI staining, (**D**) merged channels show perinuclear localization of ZIKV. Bar = 100 µm. (**E**) Percentage of ZIKV infected cells. (**F**) RT-PCR analysis of ZIKV RNA extracted from mock and ZIKV-infected neurospheres after 3 DIV, showing amplification only in infected cells.

Fig. 2. ZIKV alters morphology and halts the growth of human neurospheres

(**A**) Control neurosphere displays spherical morphology after 3 DIV. (**B**) Infected neurosphere showed morphological abnormalities and cell detachment after 3 DIV. (**C**) Culture well-plate containing hundreds of mock neurospheres after 6 DIV. (**D**) ZIKV-infected well-plate (MOI = 0.025) containing only few neurospheres after 6 DIV. Bar = 250 µm (A-B) and 1 cm (E). Quantification of the number of neurospheres in different MOI. Data presented as mean ± SEM, n=3, ***$p<0.001$

Fig. 3. ZIKV induces death in human neurospheres

Ultrastructural images of mock- and ZIKV-infected neurospheres after 6 days *in vitro*. (**A**) Well rounded mock-infected neurosphere, (**B**) ZIKV-infected neurosphere pyknotic nucleus, swollen mitochondria, smooth membrane structures and viral envelopes (arrow). Arrows point viral envelopes on cell surface (**C**), inside mitochondria (**D**), endoplasmic

PeerJ Preprints | https://doi.org/10.7287/peerj.preprints.1817v3 | CC-BY 4.0 Open Access | rec: 13 Mar 2016, publ: 13 Mar 2016

reticulum (**E**), and close to smooth membrane structures (**F**). Bar = 1 µm (A-B) and 0.2 µm (C-F). m = mitochondria; n = nucleus; sms = smooth membrane structures.

Fig. 4. ZIKV reduces the growth rate of human cerebral organoids

(**A, B**) ZIKV-infected brain organoids show reduction in growth compared with mock brain organoids. (**C, D**) 11 days after infection *in vitro*, area of 6 mock brain organoids **(**C**)** and 6 ZIKV-infected brain organoids **(**D**)** was measured before and after infection. **(E)** Quantification of the average of organoid area in 46 days *in vitro*. Data presented as mean ± SEM, Student's t-test, *p < 0.01. Arrows point to detached cells.

Fig. 5. Summary of the effects of ZIKV infection in human neural stem cells, formation of neurospheres and growth of brain organoids.

PeerJ Preprints | https://doi.org/10.7287/peerj.preprints.1817v3 | CC-BY 4.0 Open Access | rec: 13 Mar 2016, publ: 13 Mar 2016

Figure 1

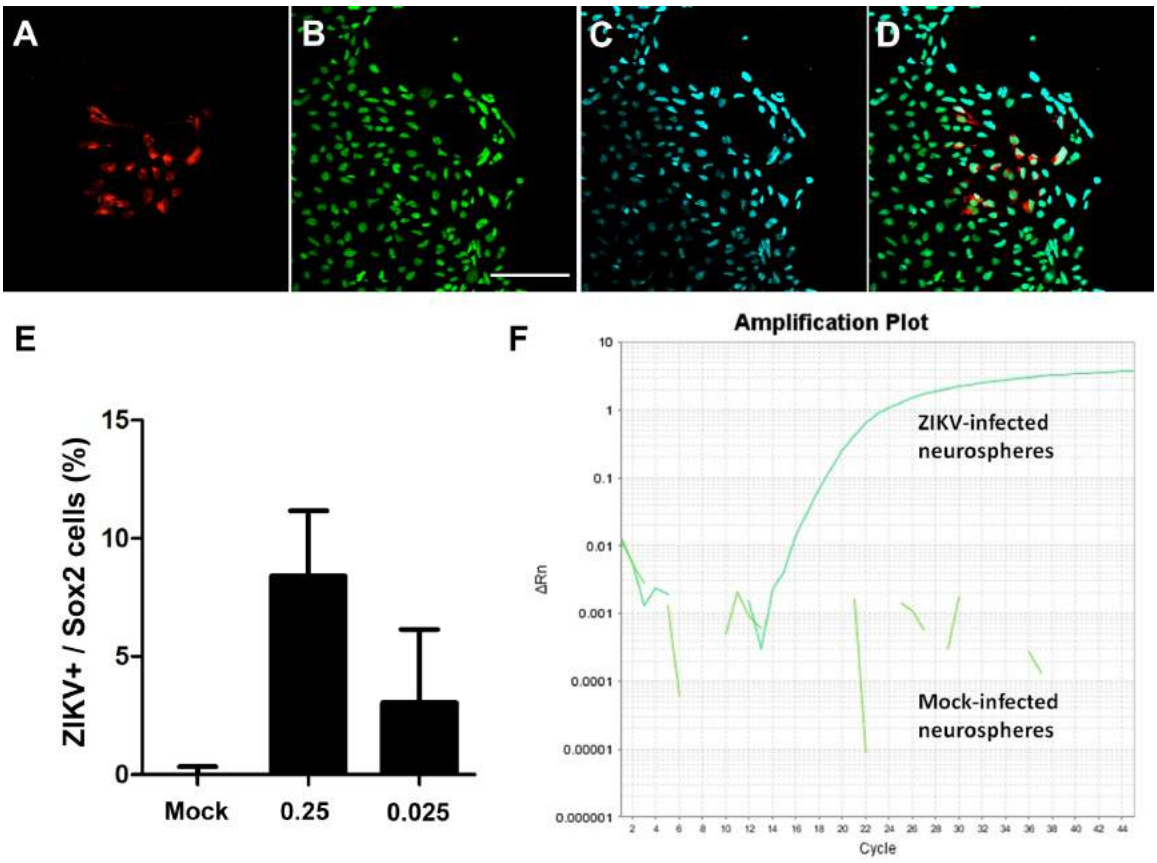

PeerJ Preprints | https://doi.org/10.7287/peerj.preprints.1817v3 | CC-BY 4.0 Open Access | rec: 13 Mar 2016, publ: 13 Mar 2016

Figure 2

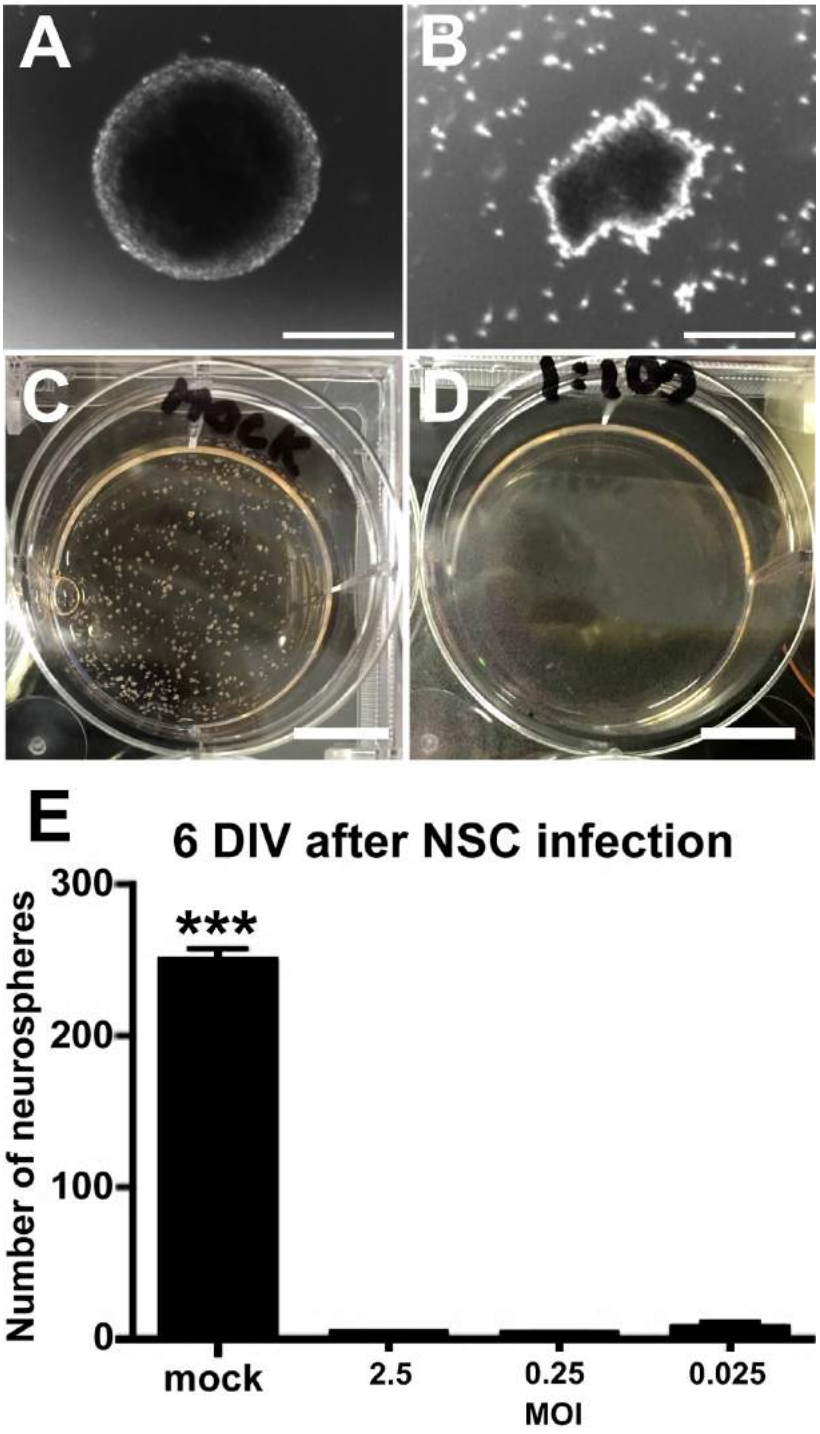

PeerJ Preprints | https://doi.org/10.7287/peerj.preprints.1817v3 | CC-BY 4.0 Open Access | rec: 13 Mar 2016, publ: 13 Mar 2016

Figure 3

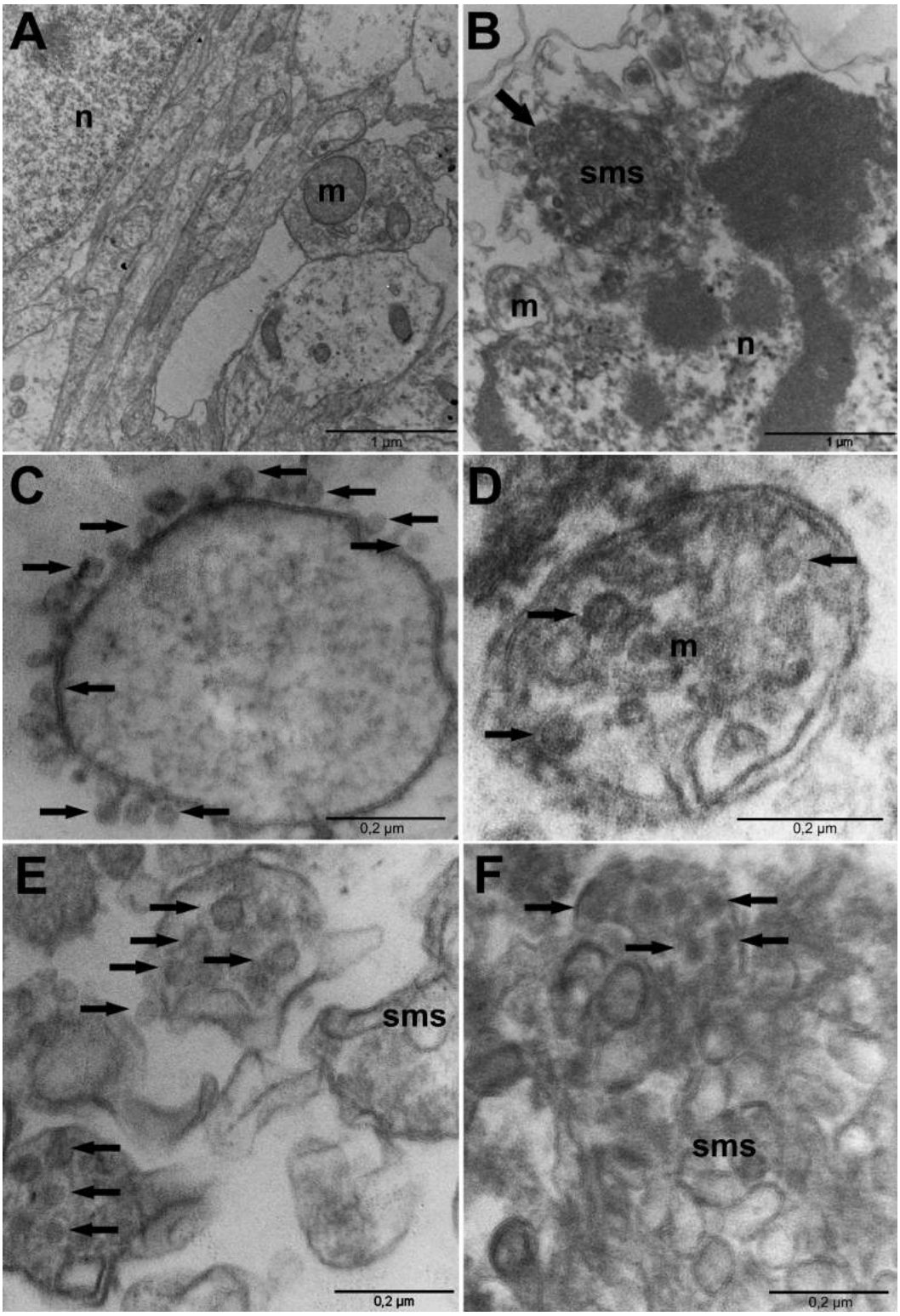

PeerJ Preprints | https://doi.org/10.7287/peerj.preprints.1817v3 | CC-BY 4.0 Open Access | rec: 13 Mar 2016, publ: 13 Mar 2016

Figure 4

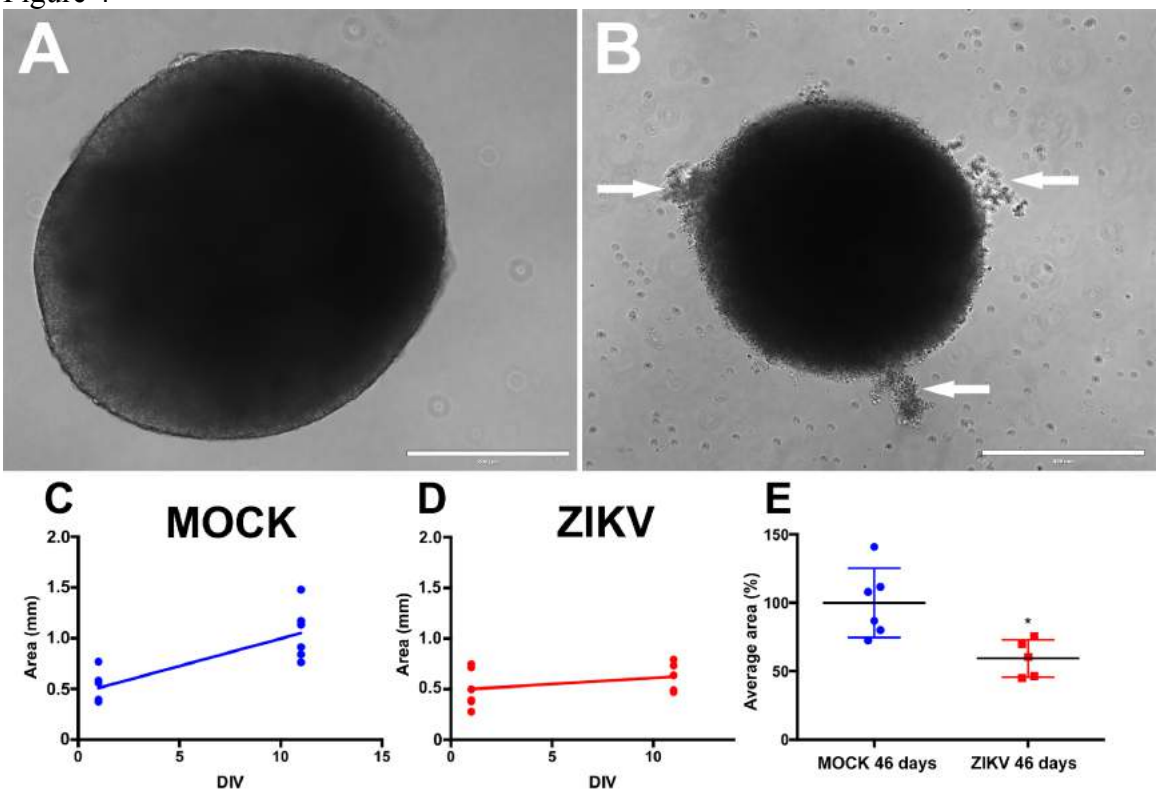

PeerJ Preprints | https://doi.org/10.7287/peerj.preprints.1817v3 | CC-BY 4.0 Open Access | rec: 13 Mar 2016, publ: 13 Mar 2016

Figure 5

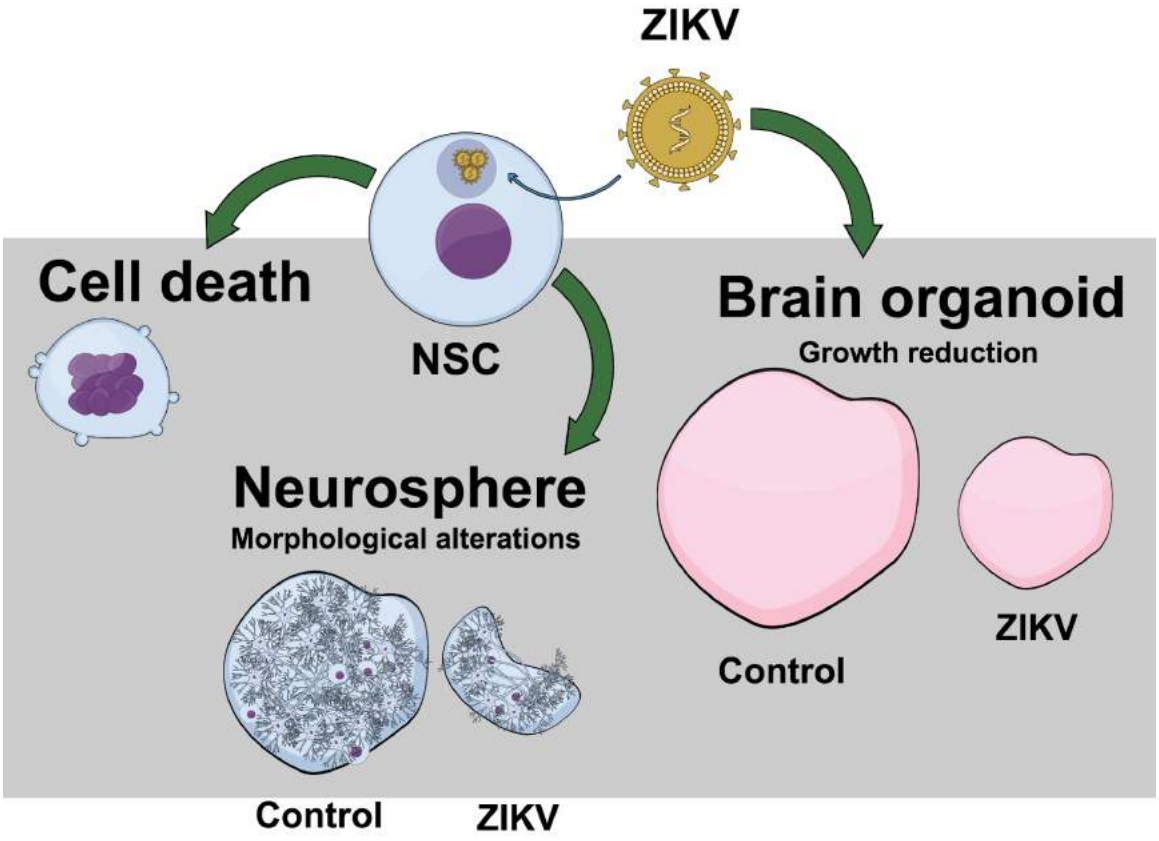

PeerJ Preprints | https://doi.org/10.7287/peerj.preprints.1817v3 | CC-BY 4.0 Open Access | rec: 13 Mar 2016, publ: 13 Mar 2016